Jurnal Polimesin
Department of Mechanical Engineering
State Polytechnic of Lhokseumawe
http://e-jurnal.pnl.ac.id/polimesin
e-ISSN : 2549-1999 No. : 6 Month : December
p-ISSN : 1693-5462 Volume : 22 Year : 2024

Article Processing Dates: Received on 2024-11-14, Reviewed on 2024-12-08, Revised on 2024-12-12, Accepted on 2024-12-15 and Available online on 2024-12-30

Interfacial stress distribution analysis of natural fiber-reinforced epoxy composites: a finite element approach

Ikramullah Ikramullah[1], Reja Gapatra[2], Seprian Haris Ananda[3], Rudi Kurniawan[1], Syarizal Fonna[1], Samsul Rizal[1], Syifaul Huzni[1,*]

[1]Department of Mechanical and Industrial Engineering, Universitas Syiah Kuala, Darussalam, Banda Aceh 23111, Indonesia

[2]PT. Pertamina Hulu Rokan, Pangkalan Susu, Sumatra Utara, Indonesia

[3]PT. Perkebunan Nusantara IV Regional 1, Medan, Sumatra Utara, Indonesia

*Corresponding author: syifaul@usk.ac.id

Abstract

The strength of fiber-reinforced composites is greatly influenced by the bonding at the fiber-matrix interface. Experimental methods to study this interface are often challenging, making numerical approaches essential for evaluating the interfacial behavior in fiber-reinforced composites. This study investigates the stress and strain distribution in the fiber, matrix, and fiber-matrix interface regions of natural fiber-reinforced single-fiber composites under tensile loading using the finite element method. Interface conditions were modeled using cohesive elements, with the composites represented in two dimensions through ABAQUS 6.14 software. The tie constrains contact model was employed to define binding interactions between the cohesive element, the fiber, and the matrix. The maximum stress value resulting from the simulation process is 202 MPa and a strain of 0.0449 mm. The stress is effectively distributed to the fiber, demonstrating that the cohesive element used in composite analysis under tensile loading serves as a reliable link between the fiber and the matrix. The simulation results revealed a maximum stress value of 202 MPa and a corresponding strain of 0.0449 mm. The stress distribution effectively transferred to the fiber, demonstrating the capability of cohesive elements to represent the interfacial bond in composites under tensile loading. These findings confirm that cohesive element modeling is reliable method for analyzing fiber-matrix interactions in natural fiber reinforced composites, providing insights for optimizing composite performance.

Keywords:

Composites, natural fibers, finite element method, cohesive elements.

1 Introduction

In recent years, synthetic fiber-reinforced polymer composites have become an effective alternative to conventional construction materials due to several factors: higher strength, higher fatigue strength, good impact energy absorption, corrosion resistance, and longer life [1]. However, due to the non-degradable nature of synthetic fibers, many studies currently want to develop natural fibers as reinforcement for composite materials [2][3][4]. Some natural fibers researched as composite reinforcement include palm fiber, bagasse fiber, ramie, and banana fiber [5][6][7][8]. One of the natural fibers that also has the potential to be used as a composite reinforcement is *Typha spp*. fiber [9].

Several factors affect composite strength, including fiber, matrix, and the strength of the interface between fiber and matrix. Fiber serves as a reinforcement that has less ductile properties but is more rigid or not easily changed. The matrix has more ductile properties but has lower strength. The strength of the interface between the fiber and the matrix plays a major role in determining the mechanical characteristics of the composite [10]. Good interface strength criteria must be able to transfer load efficiently to the fiber and maintain the interface condition between the fiber and matrix to remain bonded [11].

In the process of analyzing fiber composites, several problems are often experienced by researchers, namely the strength of the fiber-matrix interface, which is difficult to identify experimentally, so numerical simulation research using the finite element method has been used to simplify the investigation of the bonding characteristics at the interface between the fiber and matrix [12].

Previously, research has been carried out on the characteristics of single fiber, and matrix interfaces in jute fiber reinforced single fiber composites using the finite element method and experiments. The results of his research show that the results of the fragmentation test pattern carried out experimentally are close to the results in simulation with the finite element method [13]. In addition, research has also been conducted on non-linear mechanical behavior and bio-composite modeling of palm mesocarp fibers. In modeling this palm mesocarp, the study was carried out using ABAQUS software with two types of contact: frictional contact for treated fibers and tie constraints for untreated fibers [14].

Several composite simulations have been carried out under tensile loading. Prasad et al. analyzed the tensile strength simulation of a natural FRP hybrid composite of jute and banana by FEA using the SolidWorks and Analysis System (ANSYS) software package. Boundary conditions and material parameters were set for tensile test conditions [15]. Finite element analysis using the RVE method was applied to observe the random orientation and volume fraction of fibers in carbon/glass FRP hybrid composites. The randomly arranged fibers did not depict a significant impact on their tensile strength [16]. Numerical simulations based on the tensile properties of FRP hybrid composites consider the assumption of regular distribution of fiber reinforcement in the matrix. This method involves the use of RVE. The matrix properties were set as isotropic and elastic/plastic to simulate the tensile characteristics of FRP hybrid composites. Using ANSYS software, finite element simulations were also performed at various mass fractions of fiber reinforcement. From the results obtained, the finite element data around the elastic area is similar to the experimental results, unlike inside the plastic region. It was observed that at high strains, the finite element model could not fully predict the tensile characteristics [17].

Perfect bonding, frictional contact, and cohesive elements have been applied in Finite Element (FE) simulations to model the mechanical behaviour of the fiber/matrix interface. However, perfect bonding is often too idealistic and may not align consistently with experimental results [18]. Frictional contact is effective and accurate for simulating the influence of interfacial properties on Natural Fiber-Reinforced Composite (NFRC) damage but presents challenges in establishing a direct relationship between contact properties and interfacial behaviour. The cohesive element method, on the other hand, offers a more efficient and practical approach to analyzing the influence of interface properties on mechanical behaviour. By adjusting stiffness parameters and damage criteria, this method is easily implemented in FE software [19], [20]. This study employs the cohesive element method to model the mechanical behavior of *Typha spp*. fiber-reinforced single-fiber composites. Unlike

previous works that primarily relied on perfect bonding or frictional contact, this research focuses on using cohesive elements to evaluate stress and strain distribution in the fiber, matrix, and fiber-matrix interface regions under tensile loading. This approach provides a more realistic and detailed understanding of the interfacial behavior, which has been minimally explored for *Typha spp*. fibers. The cohesive element method can effectively model the mechanical behavior of the fiber/matrix interface in *Typha spp*. fiber-reinforced composites under tensile loading. Specifically, it is hypothesized that the cohesive element approach *provides* a more realistic representation of the interfacial stress and strain distribution compared to traditional perfect bonding or frictional contact methods. The main objective of this research is to analyze the stress and strain distribution in the *Typha spp*. fiber-reinforced single-fiber composite under tensile loading using the finite element method. The study aims to contribute to a deeper understanding of the interfacial behavior of natural fiber composites, offering insights into optimizing composite performance through advanced simulation techniques.

2 Materials and Methods

The research process, including pre-processing, simulation, and post-processing stages, is depicted in the flow chart shown in Fig. 1. The dimensions of the tensile test specimens used in this study refer to the standard (ASTM D638-02a). The shape and dimensions of the model are shown in Fig. 2. The database model used is the standard/explicit model or static general analysis using the 2D planar deformable model. The specimen drawing process is divided into 5 parts: upper matrix, lower matrix, fiber, upper cohesive, and lower cohesive. Furthermore, the five parts are assembled to combine all the parts that have been drawn.

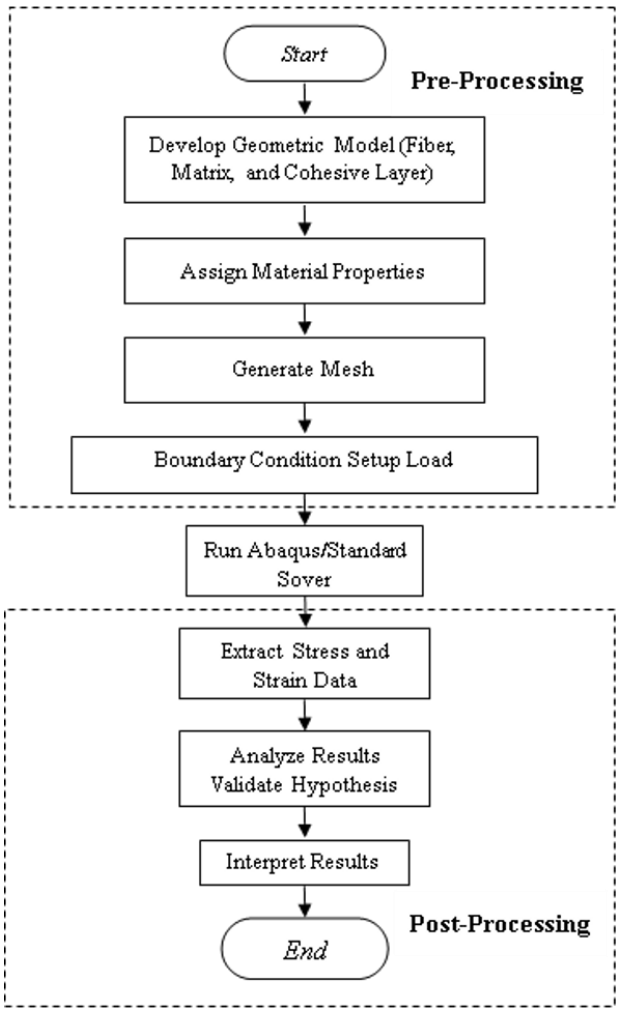

Fig. 1. The research flowchart.

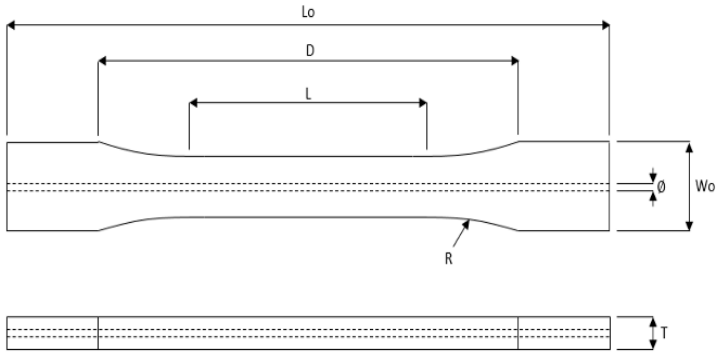

Width of narrow section (W)	13 mm
Length of narrow section (L)	57 mm
Width overall (WO)	19 mm
Length overall (LO)	165 mm
Gage length (G)	50 mm
Distance between grips (D)	115 mm
Radius of the fillet (R)	76 mm
Thickness (T)	7 mm
Fiber Diameter	1.25 mm

Fig. 2. Tensile test specimen geometry.

Table 1. Mechanical properties data of *Typha spp*. fiber and epoxy resin

Properties	*Typha spp.* [21], [22]	Epoxy [23]
Young's modulus (MPa)	11565	5000
Tensile strength (MPa)	202	73
Density (g/cm^3)	1.25	1.16
Poison ratio	0.35	0.4

The interply interface is simulated with a cohesive zone model, whose constitutive response is defined in a bi-linear traction separation law that relates the separation displacement between the upper and lower surfaces of the element to the traction vector acting on it [24]. There are several types of contact available in ABAQUS, but in this study, the type of contact that will be used is tie constrain. In this process, ABAQUS provides two choices of regions, namely the master surface, which is the critical part while the slave surface is the bound part. In this case, the m-surface is the matrix surface and fiber surface, while the s-surface is the cohesive surface that interacts with the matrix and fiber. The cohesive properties nominal stress is 10 MPa maximum damage for normal-only mode, first direction, and the second direction. Damage evolution traction 0.1 displacement at failure, and the cohesive thickness is 100 GPa.

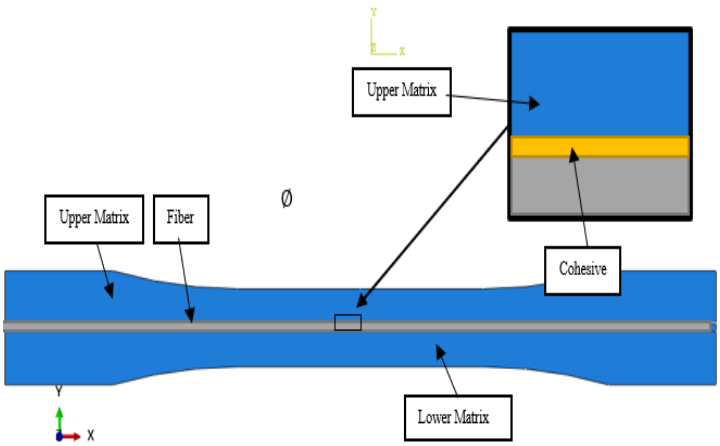

Fig. 3. 2D geometry of single fiber composite specimen.

Boundary conditions are applied so that the movement of the tensile test specimen does not move freely and the movement is as

desired. The boundary condition used is the ENCASTRE type (U1= U2 = U3 = UR1 = UR2 = UR3 = 0) given to the part of the specimen that does not move and the initial displacement on the part to be pulled. The type of load given in the simulation process is the displacement with a movement of 3 mm/minute. Boundary conditions and loading are shown in Fig. 4. The matrix mesh size is 1.5 mm, and the fiber mesh size is 1 mm. The type of mesh used is hexahedron mesh. The shape and size of the mesh used are shown in Fig. 5.

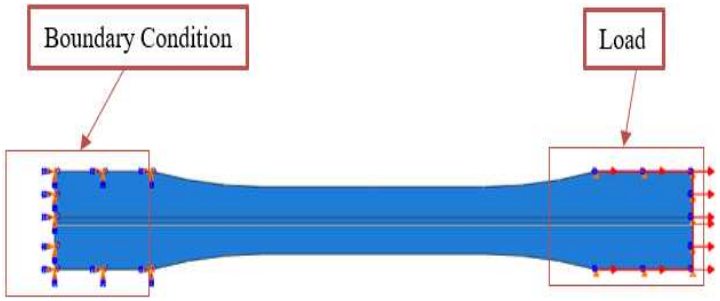

Fig. 4. Boundary conditions and loads.

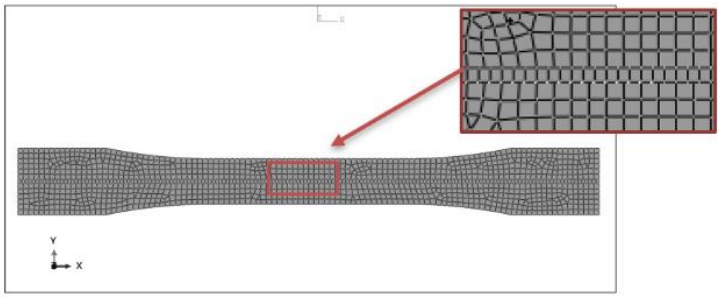

Fig. 5. Fiber and matrix meshing results in ABAQUS.

3 Results and Discussion

The results of stress simulations on single-fiber composites reinforced with *Typha spp*. Fibers using the finite element method can be seen in Fig. 6. The stress simulations performed using the finite element method show that the maximum stress value occurs in the fiber. This phenomenon can be observed in Fig. 6 by the red contour that occurs at the fiber. As can be seen, the stress is properly transferred from the transition zone to the fiber and embedded cell matrix. This explains where the reinforcing material is the stronger component, intended to carry the load received. Research by Lei Yang et al. [24] also obtained similar results, where stress was properly transferred from the transition zone to the fibers and matrix. The fibers are all tensile, with the axial stress increasing from top to bottom. However, the maximum axial stress of the fiber is still much lower than the longitudinal tensile strength of the fiber, so fiber breakage will not be induced. Thus, based on the results of simulations run using the finite element method on single fiber composites reinforced with *Typha spp*. Fibers have an excellent ability to withstand and continue the load received by the composite.

The difference in stress values experienced by the matrix and fibers can be observed in Fig. 7, which shows the maximum stress values experienced by the fiber and matrix. In the von mises stress graph for fiber and matrix, it can be seen that the maximum stress peak experienced by the fiber and matrix occurs in the middle of the specimen. In the matrix, the maximum stress value occurs along a distance of 50 mm to 130 mm with a stress value of 73 MPa.

In comparison, in the fiber, the maximum stress value occurs along a distance of 60 mm to 120 mm with a stress value of 202 MPa, which is the length of the narrow section of the tensile test specimen. For the matrix, the maximum stress value of 73 MPa is observed over a distance of 50 mm to 130 mm, reflecting the region where the matrix bears the load transferred from the fiber. The relatively lower stress in the matrix compared to the fiber can be attributed to its lower stiffness and strength, which causes it to deform more under the same applied load. In contrast, the fiber experiences significantly higher stress, with a maximum value of 202 MPa occurring along a distance of 60 mm to 120 mm. This is consistent with the fiber's role as the primary load-bearing component in the composite.

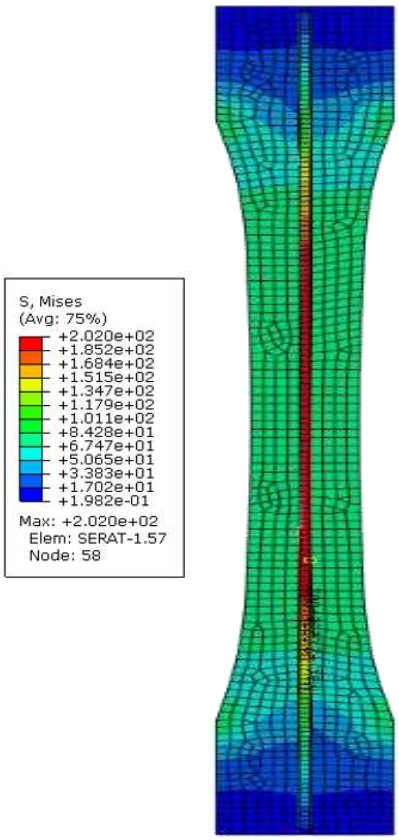

Fig. 6. Stress distribution in composite.

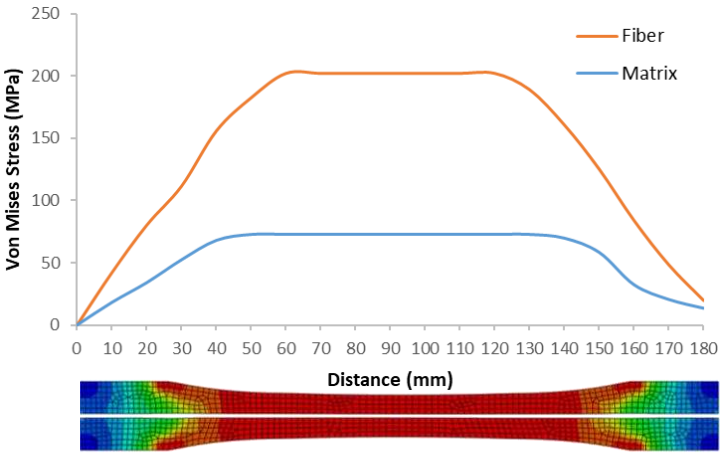

Fig. 7. (a) Von mises stress in the matrix (b) Von mises stress in the fiber.

The von Mises stress distribution in the top and bottom cohesive layers, as shown in Fig. 8, exhibits a fluctuating pattern with stress peaks and troughs along the length of the cohesive interface. The maximum von Mises stress observed is approximately 22 MPa, while the minimum stress is 0 MPa. Stress peaks occur at distances of 30 mm, 60 mm, 120 mm, 150 mm, and 180 mm, indicating regions of higher interfacial strain concentration potentially caused by local geometric or material non-uniformities. The cohesive interface plays a critical role as the primary zone for stress transfer between the fiber and matrix, and these peaks may represent locations where damage initiation or failure is likely to occur under tensile loading. In the case of single fiber composite analysis with tensile loading, the cohesive is the thinnest component that aims to predict the damage at the

interface of fiber and matrix [25]. Slight differences between the top and bottom cohesive layers suggest minor asymmetry in stress transfer, which may result from numerical approximations or local variations in material behavior.

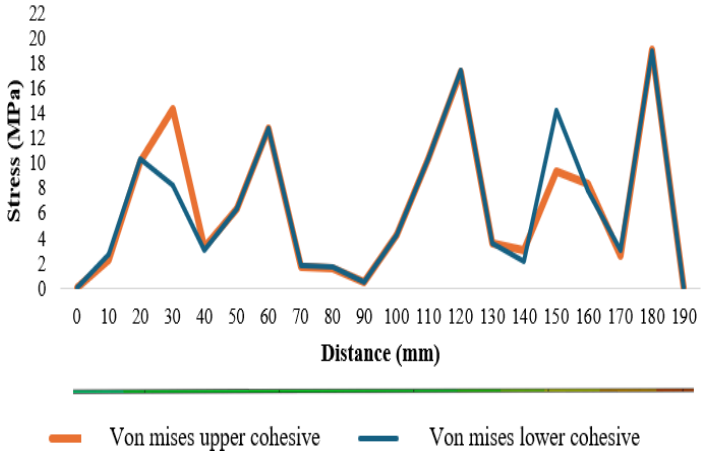

Fig. 8. Maximum stress along the cohesive.

The simulation results of strain on *Typha spp*. fiber-reinforced single-fiber composites are shown in Fig. 9. The figure shows that the maximum strain occurs in the center of the composite specimen with a maximum strain value of 0.04494. Mechanically, the tensile force received by the composite specimen rod will be evenly distributed throughout the rod's cross-section. The other side will perform the same reaction so that the additional length will occur in the middle of the specimen. The comparison of values in the matrix and fiber looks similar, as shown in Fig. 10. The figure shows that the maximum strain value on the fiber and matrix occurs at a distance of 90 mm right in the middle of the specimen.

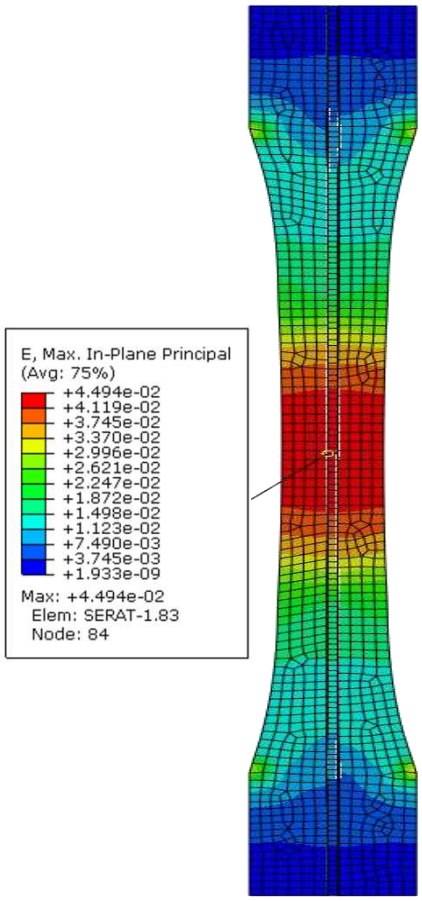

Fig. 9. Strain distribution along the specimen.

The strains that occur in the cohesive can be seen in Fig. 10. The strain graph on the cohesive shows the maximum value difference between the upper and lower cohesive. The upper cohesive shows that the maximum strain value occurs at the right end at a distance of 160 mm from the support with a strain of 0.021. In comparison, for the lower cohesive the maximum strain occurs on the left side of the cohesive at a distance of 30 mm from the support with a strain of 0.025 (Fig. 11).

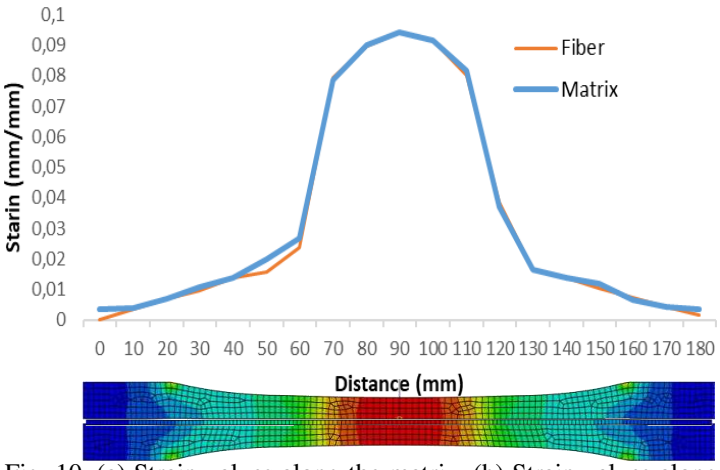

Fig. 10. (a) Strain values along the matrix, (b) Strain values along the fiber.

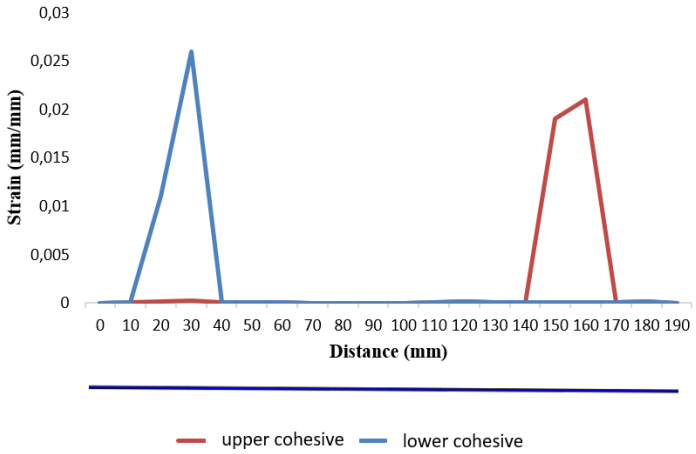

Fig. 11. Strain values along the cohesive.

The graph of the relationship between stress and strain of *Typha spp*. fiber-reinforced single-fiber composites based on simulation results can be seen in Fig. 12. Based on the chart, the elastic region is expressed by the straight part of the relationship, and the gradient is defined as the elastic modulus. In the mechanical testing of materials, the desired thing from the material is to have a significant material ductility because the greater the flexibility, it will be safer against the possibility of fracture. In addition, the material's ductility also states the energy distributed by the material to the maximum value of the material.

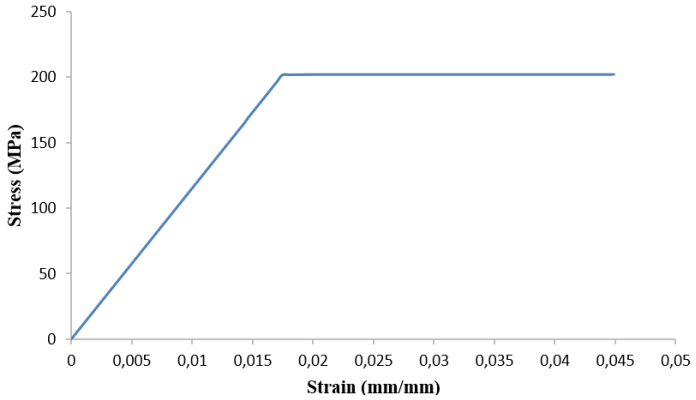

Fig. 12. Stress vs. strain diagram.

The stress-strain relationship graph in the case of *Typha spp*. fiber-reinforced single-fiber composite testing shows that the

material's ductility occurs up to the maximum point of the material with a strain value of up to 0.0174. After reaching the elastic limit point, there is no significant increase in stress, so the finite element method considers the single fiber composite to have a maximum stress value of 202 MPa with a strain of 0.0174.

Shear stress can occur when the force is deformed parallel to the surface, while in the case of the tensile test; the deformation force is applied perpendicular to the surface. The shear stress distribution contour that occurs in the case of tensile testing can be observed in Fig. 13. This figure shows that the part of the composite that experiences the most extensive shear stress distribution occurs in the matrix part of the composite. There is a difference in the direction of the shear force received by the specimen, where for the blue contour, the shear force is negative, while for the red contour, the force direction is positive.

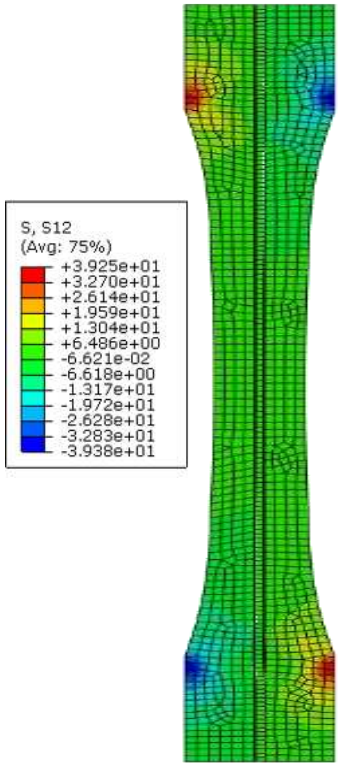

Fig. 13. Shear stress distribution along the specimen.

A graph of the shear stress experienced by the *Typha spp*. fiber-reinforced composite matrix is shown in Fig. 14. The strength of the fiber and matrix interface can be seen through the critical length of the fiber. To evaluate the critical length of the fiber, it is necessary to consider the load transfer process to the fiber through the matrix. The shear strength of the matrix and the fiber-matrix interface is required to carry the load due to friction by the fiber and matrix to obtain the interface strength. Shear stress transfers the load passed by the matrix to the fiber so the fiber can do its job as reinforcement in the composite.

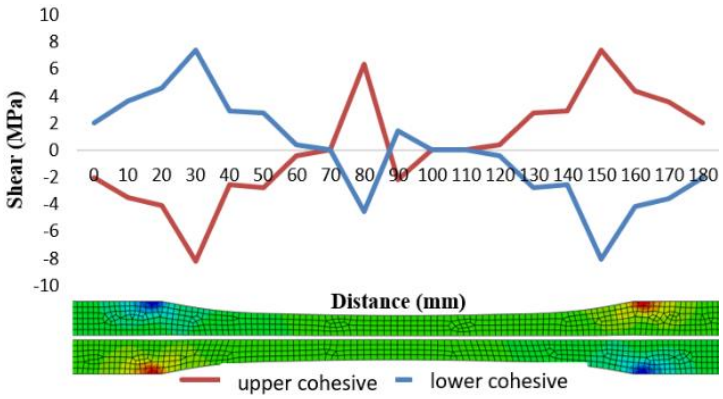

Fig. 14. Shear stress along the matrix.

In Fig. 15, it can be observed that the shear stress occurring in the upper matrix has shifted to the negative direction with a stress value of -8.19 MPa at a distance of 30 mm from the support and a distance of 80 mm from the support there is a shift to the positive direction with a stress value of 6.39 MPa, and at a distance of 150 mm from the support the shear stress increases to 7.42 MPa in the positive direction. Another case occurs in the lower matrix, where the shear stress acting at 30 mm from the support shifts to a positive direction with a stress value of 7.38 MPa; at a distance of 80 mm from the support, the stress shifts to a negative direction with a stress value of -4.53 MPa and at a distance of 150 mm from the support the shift value moves to a negative trend with a stress value of -8.08 MPa. In Fig. 14, the shear stress acting on the fiber can be observed, where two shear stresses are acting at 20-30 mm and 150-160 mm from the support.

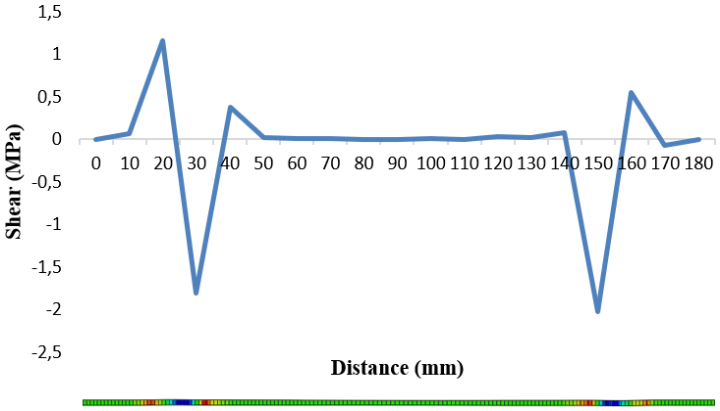

Fig. 15. Shear stress along the fiber.

In the case of fiber composites, it can be seen that the shear stress that occurs is a double shear stress where more than one plane shear occurs, namely between the fiber plane and the matrix plane. In the case of single fiber composites, when a load is applied, a highly irregular stress occurs at the fiber interface and matrix interface. The average nominal intensity of these stresses is obtained by dividing the force received by the cohesive projected area of the specimen. The shear stress that occurs at the interface (cohesive) between the fiber and matrix can be seen in Fig. 16.

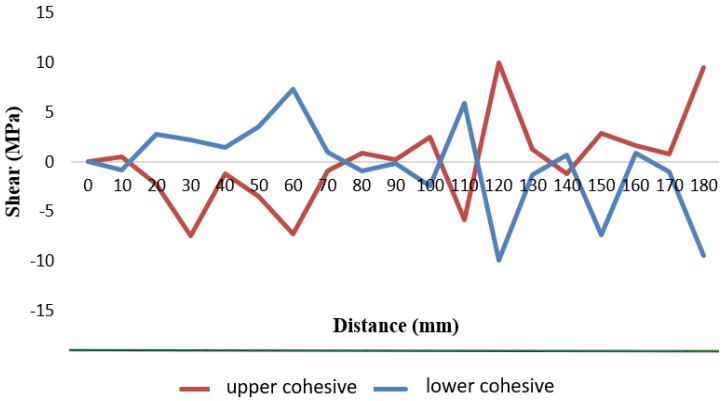

Fig. 16. Shear stress values along cohesive.

4 Conclusion

In conclusion, there must be no reference. The simulation of *Typha spp*. fiber-reinforced single-fiber composites using the finite element method have been successfully conducted. The maximum von mises stress distribution received in the *Typha spp*. The fiber-reinforced single-fiber composite specimen is 202 MPa, and the maximum strain received by the composite model is 0.04494 mm/mm. It can be concluded that the use of cohesive elements be used to analyze the interface condition of the fiber and matrix of the composite.

References

[1] Z. N. Azwa, B. F. Yousif, A. C. Manalo, and W. Karunasena, "A review on the degradability of polymeric composites based on natural fibres," *Mater Des*, vol. 47, pp. 424–442, Mar. 2013.

[2] F. Yudhanto, V. Yudha, Jamasri, and A. Wisnujati, "Effect of alkali soaking time on physical and morphological properties of Agave cantala fiber," *AIP Conf Proc*, vol. 2499, no. 1, p. 040002, Nov. 2022, doi: 10.1063/5.0104998.

[3] E. Contini *et al.*, "Isolation of cellulose from salacca midrib fibers by chemical treatments," *IOP Conf Ser Mater Sci Eng*, vol. 434, no. 1, p. 012078, Nov. 2018.

[4] Akram Tamlicha, S. Rizal, I. Hasanuddin, M. M. Noor, I. Ikramullah, and N. Nazaruddin, "The Simulation Of Drop-Weight Impact Test On Ramie-Eglass Hybrid Fiber Composite For Jaloe Kayoh Wall Material," *Jurnal Polimesin*, vol. 22, no. 1, pp. 75–82, Feb. 2024.

[5] T. A. Adlie, N. Ali, S. Huzni, I. Ikramullah, and S. Rizal, "Impact of Zinc Oxide Addition on Oil Palm Empty Fruit Bunches Foamed Polymer Composites for Automotive Interior Parts," *Polymers 2023, Vol. 15, Page 422*, vol. 15, no. 2, p. 422, Jan. 2023.

[6] M. Iqbal, M. S. Satrianda, T. Firsa, S. A. Azan, and L. B. Abhang, "Bending Strength of Fiber Metal Laminate Based on Abaca Fiber Reinforced Polyester and Aluminum Alloy Metal Sheet," *Key Eng Mater*, vol. 892, pp. 134–141, 2021.

[7] D. G. Devadiga, K. S. Bhat, and G. T. Mahesha, "Sugarcane bagasse fiber reinforced composites: Recent advances and applications," *Cogent Engineering*, vol. 7, no. 1, Jan. 2020.

[8] I. Mawardi, S. Rizal, S. Aprilia, and M. Faisal, "Kajian stabilitas termal bahan baku material insulasi panas berbasis serat alam: kayu kelapa sawit dan serat rami," *Jurnal Polimesin*, vol. 19, no. 1, pp. 16–21, Feb. 2021.

[9] S. Huzni *et al.*, "The Role of Typha angustifilia Fiber–Matrix Bonding Parameters on Interfacial Shear Strength Analysis," *Polymers 2022, Vol. 14, Page 1006*, vol. 14, no. 5, p. 1006, Mar. 2022.

[10] N. Karthi, K. Kumaresan, S. Sathish, S. Gokulkumar, L. Prabhu, and N. Vigneshkumar, "An overview: Natural fiber reinforced hybrid composites, chemical treatments and application areas," *Mater Today Proc*, vol. 27, pp. 2828–2834, Jan. 2020.

[11] T. E. S. de Lima, A. R. G. de Azevedo, M. T. Marvila, V. S. Candido, R. Fediuk, and S. N. Monteiro, "Potential of Using Amazon Natural Fibers to Reinforce Cementitious Composites: A Review," *Polymers 2022, Vol. 14, Page 647*, vol. 14, no. 3, p. 647, Feb. 2022.

[12] X. Xiong *et al.*, "Finite element models of natural fibers and their composites: A review," *Journal of Reinforced Plastics and Composites*, vol. 37, no. 9, pp. 617–635, May 2018.

[13] C. Guillebaud-Bonnafous, D. Vasconcellos, F. Touchard, and L. Chocinski-Arnault, "Experimental and numerical investigation of the interface between epoxy matrix and hemp yarn," *Compos Part A Appl Sci Manuf*, vol. 43, no. 11, pp. 2046–2058, Nov. 2012.

[14] S. H. Hanipah, M. A. P. Mohammed, and A. S. Baharuddin, "Non-linear mechanical behaviour and bio-composite modelling of oil palm mesocarp fibres," *Composite Interfaces*, vol. 23, no. 1, pp. 37–49, Jan. 2015.

[15] V. Prasad, A. Joy, G. Venkatachalam, S. Narayanan, and S. Rajakumar, "Finite Element Analysis of Jute and Banana Fibre Reinforced Hybrid Polymer Matrix Composite and Optimization of Design Parameters Using ANOVA Technique," *Procedia Eng*, vol. 97, pp. 1116–1125, Jan. 2014.

[16] S. Banerjee and B. v. Sankar, "Mechanical properties of hybrid composites using finite element method based micromechanics," *Compos B Eng*, vol. 58, pp. 318–327, Mar. 2014.

[17] M. D. Shokrian, K. Shelesh-Nezhad, and B. H Soudmand, "Numerical Simulation of a Hybrid Nanocomposite Containing Ca-CO3 and Short Glass Fibers Subjected to Tensile Loading," *Mechanics Of Advanced Composite Structures*, vol. 4, no. 2, pp. 117–125, Nov. 2017.

[18] D. Zhang, N. R. Milanovic, Y. Zhang, F. Su, and M. Miao, "Effects of humidity conditions at fabrication on the interfacial shear strength of flax/unsaturated polyester composites," *Compos B Eng*, vol. 60, pp. 186–192, Apr. 2014.

[19] M. Linke and R. Lammering, "On the calibration of the cohesive strength for cohesive zone models in finite element analyses," *Theoretical and Applied Fracture Mechanics*, vol. 124, p. 103733, Apr. 2023.

[20] X. Xiong *et al.*, "Finite element models of natural fibers and their composites: A review," *Journal of Reinforced Plastics and Composites*, vol. 37, no. 9, pp. 617–635, May 2018.

[21] A. Witztum and R. Wayne, "Fibre cables in the lacunae of Typha leaves contribute to a tensegrity structure," *Ann Bot*, vol. 113, no. 5, pp. 789–797, 2014.

[22] S. Rizal *et al.*, "Tailoring the Effective Properties of Typha Fiber Reinforced Polymer Composite via Alkali Treatment," *BioResources*, vol. 14, no. 3, pp. 5630-5645, 2019.

[23] J. M. L. dos Reis, "Effect of temperature on the mechanical properties of polymer mortars," *Materials Research*, vol. 15, no. 4, pp. 645–649, Jul. 2012.

[24] L. Yang, Z. Wu, D. Gao, and X. Liu, "Microscopic damage mechanisms of fibre reinforced composite laminates subjected to low velocity impact," *Comput Mater Sci*, vol. 111, pp. 148–156, Jan. 2016.

[25] W. G. Jiang, R. Z. Zhong, Q. H. Qin, and Y. G. Tong, "Homogenized Finite Element Analysis on Effective Elastoplastic Mechanical Behaviors of Composite with Imperfect Interfaces," *International Journal of Molecular Sciences*, vol. 15, no. 12, pp. 23389–23407, Dec. 2014.